A Journal of the Gesellschaft Deutscher Chemiker

Angewandte International Edition GDCh Chemie

www.angewandte.org

Accepted Article

Title: The electron spin as a chiral reagent

Authors: Ron Naaman, Tzuriel S. Metzger, Suryakant Mishra, Brian P. Bloom, Naama Goren, Avner Neubauer, Guy Shmul, Jimeng Wei, Shira Yochelis, Francesco Tassinari, Claudio Fontanesi, David H. Waldeck, and Yossi Paltiel

To be cited as: *Angew. Chem. Int. Ed.* 10.1002/anie.201911400
Angew. Chem. 10.1002/ange.201911400

Link to VoR: http://dx.doi.org/10.1002/anie.201911400
http://dx.doi.org/10.1002/ange.201911400

WILEY-VCH

10.1002/anie.201911400

The electron spin as a chiral reagent

Tzuriel S. Metzger,[a#] Suryakant Mishra,[b#] Brian P. Bloom,[d#] Naama Goren,[a] Avner Neubauer,[a] Guy Shmul,[e], Jimeng Wei, [d] Shira Yochelis,[a] Francesco Tassinari,[b] Claudio Fontanesi,[c] David H. Waldeck,[d*] Yossi Paltiel,[a*] Ron Naaman[b*]

a) Applied Physics Department and the Center for Nano-Science and Nano-Technology, The Hebrew University of Jerusalem, Jerusalem, 91904 Israel
b) Department of Chemical and Biological Physics, Weizmann Institute of Science, Rehovot 76100, Israel
c) Department of Engineering "Enzo Ferrari", DIEF, University of Modena and Reggio Emilia, 41125 Modena, Italy.
d) Department of Chemistry, University of Pittsburgh, Pittsburgh, Pennsylvania 15260, USA
e) Chemical Services, Weizmann Institute, Rehovot 76100, Israel

Abstract

In contrast to the notion that enantiospecific chemical reactions require a chiral reagent molecule or catalyst, this work shows that enantioselective chemical transformations can be induced by the electron spin itself. As electrons are injected from a magnetized electrode into an adsorbed molecule, they have a distinct spin orientation relative to their velocity; i.e., they have a well-defined helicity. Thus, it is possible to replace a conventional enantiopure chemical reagent by spin-polarized electrons that provide the chiral bias for enantioselective reactions. Three examples of enantioselective chemistry, resulting from electron spin polarization, are presented. The first example demonstrates enantioselective association of a chiral molecule with an achiral self-assembled monolayer film that is spin-polarized. The other two studies show that the chiral bias provided by the electron helicity can drive both reduction and oxidation enantiospecific electrochemical reactions. In each case, the enantioselectivity does not result from enantiospecific interaction of the molecule with the ferromagnetic electrode, but rather it arises from the polarized spin that crosses the interface between the substrate and the molecule. In all three cases, the direction of the electron spin polarization defines the sense (left-handed versus right-handed) of the enantioselectivity. This work demonstrates a new mechanism for realizing enantioselective chemistry.

Key words: Spin, chirality, electrochemistry, enantioselectivity, CISS

The conventional wisdom in Chemistry is that an enantiospecific chemical process requires a chiral bias. Commonly, this bias manifests as one enantiomer of a chiral reactant, a chiral catalyst, or a chiral solvent. Although it is well established that a magnetic field itself cannot provide the chiral preference,[1] using a magnetic field in conjunction with photoinduced processes can initiate an enantioselective process, e.g., magnetochiral anisotropy.[2,3] It has also been shown that a metal electrode, which is either chiral[4] or coated with chiral molecules[5,6,7] or a chiral film,[8,9] can display enantiospecific interactions with a redox couple in solution. This enantiospecificity is commonly explained by the three-dimensional spatial arrangement of the chiral surface molecule(s) and the enantiomer in solution, the "lock and key" model.[10] In other work, it has been shown that enantioselective adsorption on magnetic surfaces can be realized,[11] and it arises because the charge polarization of the adsorbing chiral molecule is accompanied by a spin polarization.[12] The present study is distinguished from this earlier work, by revealing the role of an injected electron's spin even when the electron *crosses* interfaces. We demonstrate that spin-polarized electrons can induce enantioselectivity in chemical reactions for three cases: i) enantiospecific association between chiral molecules and spin-polarized achiral molecules, ii) enantioselective electrochemical reduction and oxidation of a racemate mixture in solution, and iii) enantioselective electropolymerization of achiral monomers. In each of these examples, the chiral bias (enantioselectivity) arises from the orientation of the electron spin. While in the first case we show that the spin polarization of the ferromagnetic (FM) surface can propagate through a distance of about 0.75 nm in an achiral film, in the second example we show that transfer of spin-polarized electrons over larger distances, of about 1 nm, can induce enantioselective redox chemistry. In the third case, a helical polymer is constructed from achiral monomers so that the enantioselectivity must arise from the spin-polarized electrons of the magnetic surface. These three examples demonstrate that spin polarized electrons can substantially impact enantioselectivity and it should accompany the conventional "lock and key" model explanation.[10]

Electron spin, the intrinsic angular momentum of the electron, is an essential concept for describing the formation or disruption of chemical bonds in chemical reactions. Despite its importance, the control of chemical reactions by control of the electron spin orientation has typically been limited to unimolecular or photochemical processes.[13,14] In part, this results from the electron spin not being strongly coupled, "locked", to the molecular frame, so that the relative orientation of the reaction partners' spins is not well defined. The recently discovered chiral

induced spin selectivity (CISS) effect, in which an electron moving through a chiral molecule is spin-polarized either parallel or antiparallel to its velocity,[15,16] provides a mechanism by which the electron spin can be fixed to a molecular symmetry axis. CISS implies that electrons can be extracted (or injected) with a preferred spin orientation from chiral molecules. Moreover, it should be possible to affect the efficiency of charge transfer processes by choice of the spin orientation and molecular enantiomer.[17] Namely, one spin will be injected preferentially for one enantiomer and the opposite spin should be injected preferentially for the other enantiomer. The coupling of the electron's spin orientation to the molecular chirality opens a new approach for controlling the enantioselectivity of chemical reactions.

It is known that a spin-polarized electron can be characterized by its helicity, which is defined as $H_e = \vec{S} \cdot \vec{p}$, where $\vec{S}$ is the spin and $\vec{p}$ is the linear momentum of the electron. When $\vec{S}$ and $\vec{p}$ are parallel to each other, the helicity is right-handed, or positive; and when they are antiparallel the helicity is left-handed, or negative. A chiral molecule possesses a chiral component to its electric field, and its interaction with an electron depends on the electron's helicity; correspondingly, a spin-polarized electron interacts differently with the two different enantiomers of a chiral molecule. Indeed, the spin-polarization of electrons has been shown by transmitting photoelectrons through a chiral monolayer of double stranded DNA, which acts as a spin filter,[18] and their enantioselectivity was shown by electron-induced dissociation of chiral molecules.[19] This work shows that the spin-polarized electron can act as a "chiral reagent" to induce enantiospecific electrochemical transformations.

First we present results on the enantioselective association reaction with spin-polarized monolayers. These results serve later to prove that indeed the enantioselective process occurs by electrons that cross the chiral molecule/ferromagnetic interface. We use the spin density from a magnetized Ni surface to spin-polarize an adsorbed monolayer film, comprising achiral molecules, that gives rise to an enantiospecific interaction with (*S*)- and/or (*R*)-1-amino-2-propanol. Measurements on Hall devices show that the charge reorganization, which occurs upon association, is accompanied by a spin polarization that drives the enantiospecific interaction (see Supporting Information for more details). The magnetic substrate is an ultrathin 5 nm Ni / 10 nm Au film which is magnetized either parallel (Up) or antiparallel (Down) with the surface normal and is coated with an achiral self-assembled monolayer (SAM) of carboxyl-terminated

10.1002/anie.201911400

alkanethiols [HS-$(CH_2)_{x-1}$-COO^-] (see SI). Fig. 1A shows a schematic diagram of the experimental setup used to investigate the enantiospecific association.

The 1-amino-2-propanol:SAM adduct was monitored by infrared (IR) spectroscopy as a function of the substrate magnetization (either Up or Down) and the incubation time. Fig. 1C shows the IR absorption in the OH stretching region (3200-3500 cm^{-1}) for the S-1-amino-2-propanol after 2 minutes of exposure to a thioglycolic acid [HS-CH_2-COO^-] achiral monolayer. The spectra are shown for two different spin polarization directions of the SAM and for two different control samples without magnetization: a bare Au surface and a SAM coated Au surface. Each experiment was repeated at least three times. Fig. 1B presents IR spectra for SAMs exposed to 1mM solutions of both the (*R*)- or (*S*)-enantiomers for different interaction times. The hydroxyl stretch is clearly visible within the expected range and the transition strengths show a correlation between the chirality (*R*- / *S*-) of the 1-amino-2-propanol and the direction of the SAMs' spin polarization; the R enantiomer adsorbs more strongly under the Up magnetization and the S enantiomer adsorbs more strongly for the Down magnetization, but not necessarily at the same rate (i.e., largest enantioselectivity at 2 min. for Down and at 10 min. for Up). This selectivity persists for adsorption times up to about 30 to 45 minutes. For longer adsorption times, no discernible difference in the adsorption strengths were found.

10.1002/anie.201911400

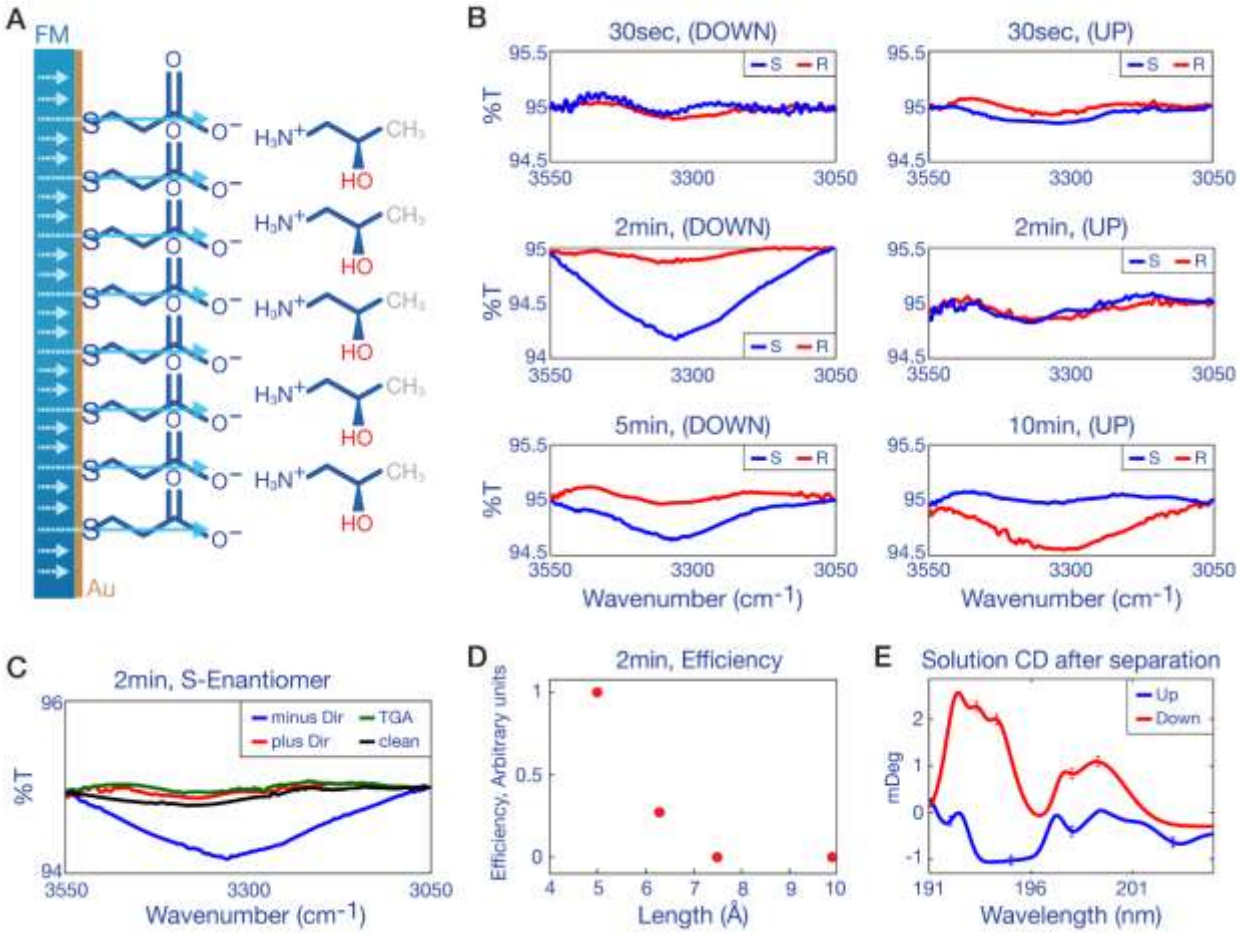

Figure 1: Enantioselective association between 1-amino-2-propanol and a carboxylate self-assembled monolayer. A) The scheme, from left to right, shows the layers on the wafer; magnetized Ni ferromagnet, Au film, thiol SAM, and bound 1-amino-2-propanol. B) FTIR spectra are shown for (*R*)- and (*S*)-enantiomers at different exposure times and magnetization directions. Note that the OH stretch appears only for the (*R*)-enantiomer with the SAM magnetized in the Up direction and for the S-enantiomer with the SAM magnetized in the Down direction. C) The image shows FTIR spectra for a clean gold surface (black), a surface with a thioglycolic acid SAM (green), and a SAM surface after reaction with the (*S*)-enantiomer of 1-amino-2-propanol under Up (red) and Down (blue) magnetization directions. D) Adsorption efficiency as a function of the achiral monolayer length. The efficiency is calculated by comparing the integrated area differences between (*S*)- and (*R*)- enantiomers under Down spin-polarization, after 2 minutes of adsorption. The efficiency was normalized to the maximum difference in area between *S* and *R* in the OH stretch region. E) Circular dichroism (CD) spectra of solutions of 1-amino-2-propanol after 1400 cycles of adsorption, transfer, and desorption. The signal shows the *enantiomeric excess* of the (*R*) molecule in solution. The CD spectra of the pure solutions, is presented in Fig. S4.

The spatial extent of the spin polarization/proximity effect on the enantioselectivity was evaluated by changing the methylene chain length of the SAM molecules, HS-$(CH_2)_n$-COO^-. The association was studied for $n = 1$ to $n = 7$, and the enantioselectivity persisted only to a linker

length of $n = 2$, which corresponds to about 6.3 Å. For mercaptobutyric acid ($n = 3$), and longer alkyl chain length (increasing *n*, i.e. number of methylenes), no selectivity was observed. This finding is shown in Fig. 1D by plotting the normalized efficiency of the adsorption (integral area differences between (*S*)- and (*R*)- enantiomers, after 2 minutes of adsorption) versus the length of the achiral SAM molecules. These results were corroborated by kinetic studies of the enantiospecific adsorption (see Table S1.) and demonstrate that the spin exchange interaction decays within 0.75 nm from the ferromagnet-gold covered surface.

The enantiospecific interactions in the association reaction were used to separate enantiomers from a racemate mixture. An autonomous machine was constructed to move the SAM coated substrate from a 'reaction vessel', in which the adsorption takes place, to a 'release vessel' in which the product is collected. In the reaction vessel, the spin-polarized, thioglycolic acid SAM is dipped into a solution containing a racemate mixture of 0.5 mM (R- / S-)-1-amino-2-propanol. Depending on the SAMs spin-polarization direction one enantiomer is adsorbed preferentially on the surface. The substrate is then moved to the release vessel (a pH 12.5 solution) in which the electrostatic bond between the 1-amino-2-propanol and the carboxylate SAM is cleaved, and the adsorbed 1-amino-2-propanol is released. Fig. 1E shows a CD spectrum for the reaction solution after this process was repeated 1400 times; an enantiomeric excess of about 20% is created in the reaction vessel for the DOWN magnetization direction. The repetitive process demonstrates a technique for continuous separation, at low pressure, for which more repetitions should improve the enantioseparation.

Next, we demonstrate that an enantioselective redox reaction can result from the spin polarization of an electron and not merely enantiospecific interaction with a FM electrode. This was shown by using the same gold coating thickness on a nickel electrode with a 1.0 nm thick self-assembled monolayer of 1-hexanethiol. Because the spin penetration from the FM into the adsorbed SAM extends no further than 0.75 nm; no enantiospecific interaction with a spin-polarized surface is expected. We investigated electrochemical oxidation and reduction reactions for R- and S- ferrocene ((*R,S*)-(+/-)-*N,N*-dimethyl-1-ferrocenylethylamine) in solution, when electrons are injected with their spin polarized parallel (magnet down) or anti-parallel (magnet up) to their velocity. The scheme in Figure 2A illustrates the experimental setup used in the current part of the work for a racemic mixture of enantiomers. Cyclic voltammetry (CV) and electrolysis experiments were performed in a three electrode electrochemical cell, for which the working

10.1002/anie.201911400

electrode is a thin (120 nm) nickel film with a 10 nm Au overcoat (more details are given in the supporting information) that is magnetized perpendicular to the electrode surface by the presence of a 0.5 T permanent magnet (see Fig. 2A).

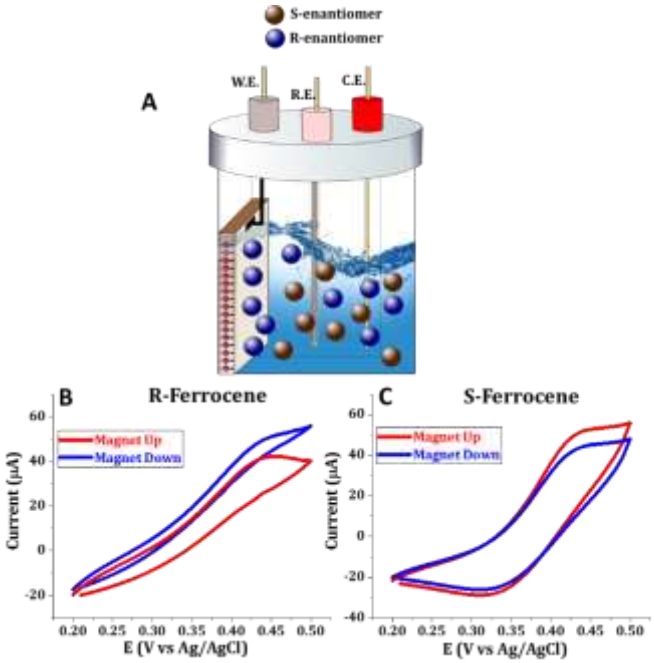

Figure 2: The experimental setup for spin-dependent electrochemical experiments. A) Illustration of an electrochemical reaction cell, in which the magnetized ferromagnetic electrode has spins oriented normal to the electrode surface. The R- and S-enantiomer (blue and grey spheres) are in the solution. B, C) Electrochemical response of R- and S- ferrocene solution with a hexanethiol coated Au/Ni ferromagnet used as the working electrode. The difference between the results in (B) and (C) are probably due to the different in purity between the two enantiomers or some change in the leakage current from the electrodes.

Figures 2B and 2C show CVs performed on solutions of the pure enantiomer, a clear dependence of the electrochemical behavior on the magnet direction (compare blue and red CV curves) is evident, even with a six alkyl carbon (1-hexanethiol) SAM on the electrode surface. This implies that the enantioselectivity is associated with the helicity of the electron, rather than an enantiospecific surface confined interaction between the molecule and the FM electrode.

The effect of spin-injection, i.e. exploiting the electron spin as a reagent, to perform an enantioselective, electrochemical reduction reaction was also investigated. Here, a racemate solution of camphorsulfonic acid (CSA) was prepared and the enantioselective electroreductive decomposition to form isoborneol was performed, see Figure 3A. Following the spin-dependent electroreduction, the enantiomeric excess of the CSA molecule in the solution was characterized by circular dichroism measurements.

10.1002/anie.201911400

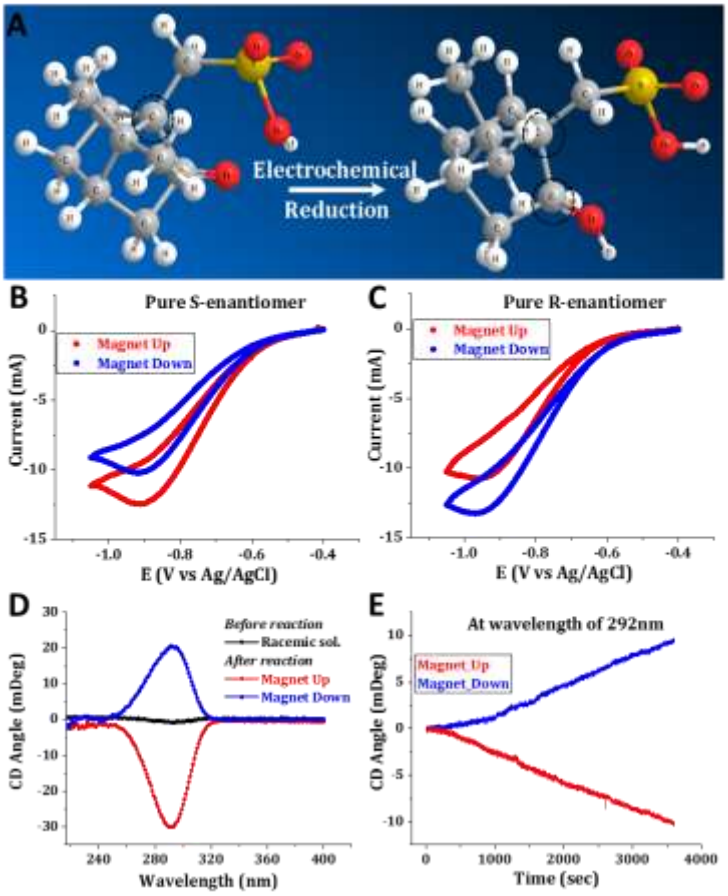

Figure 3: Enantioselective electroreduction of camphorsulfonic acid (CSA) on magnetized nickel electrodes. A) The electroreduction reaction of CSA to 10-mercaptoborneol (see details in the Methods section for more information). B&C) Cyclic voltammograms of (*S*)- and (*R*)- CSA with a Ni electrode magnetized in the Up (red) and Down (blue) orientation. D) Circular dichroism (CD) spectra of the solution following electroreduction obtained when the magnetic electrode is pointing Up (red) or Down (blue); the black spectrum shows the CD of the racemate mixture before the reaction. E) The change in the CD peak at 292 nm as a function of reaction time for the magnet oriented Up (red) and Down (blue).

Remarkably, cyclic voltammograms of an enantiomerically-pure camphorsulfonic acid solution show substantial differences in the current upon switching the direction of applied magnetization to the electrode surface (Fig. 3B and 3C). For the case of the (1*S*)-10-camphorsulfonic acid the voltammogram shows a larger current when the magnet is pointing Up (North, red) than when the magnet is rotated to point Down (South, blue). Conversely, for (1*R*)-10-camphorsulfonic acid, the current in the voltammogram is higher when the magnet is oriented Down than when the magnet is pointing Up. The effect is especially pronounced at about -0.9 V,

corresponding to the reduction peak of the CSA. The reaction product, as shown in Fig. 3A, was identified using mass-spectrometry, NMR, UV-visible absorbance, and circular dichroism (CD) spectroscopy. The results from spectroscopy were corroborated by quantum chemistry calculations of the absorption and CD spectra; see the Methods section and the Supplementary Information (SI) for more details.

Bulk electrolysis for the reduction of CSA, in a spin-dependent electrochemistry set-up (Figure 3A), was carried out in a 20 mM racemate CSA solution at a constant potential of -0.9 V vs Ag/AgCl for 360 minutes. The changes in the CD spectrum at 292 nm (Fig. 3D) correspond to a change in the *enantiomeric excess* of the solution and were found to depend on the orientation of the magnet used to magnetize the electrode. When the electrode is magnetized Up, the CD signal is negative; and when the electrode is magnetized Down, the CD signal is positive. Fig. 3E shows the change in the intensity of the CD peak at 292 nm as a function of time, for the two different magnetization directions.

The data demonstrate that spin selective electron injection can be used to perform enantioselective reduction. From the change in intensity of the absorbance spectrum of the reactant and the intensity of the CD spectrum, we find that after 6 hours of electrolysis, 6.2 mmol (~20% of the initial amount) of CSA is reduced and the enantiomeric excess in the solution is about 11.5%. Given that the initial 3 mL solution contained 10 mmol of (*R*)- and 10 mmol of (*S*)-enantiomer, 44% of the reactant conversion was the (*R*)-enantiomer and the remaining 56% was the (S)-enantiomer. Moreover, the enantiomer that appears in excess, after electrolysis, depends on the magnetization direction of the electrode. These results are consistent with the enantioselectivity in the voltammograms' Faradaic current (compare Fig. 3B and 3C): in Figure 3B the peak current (at -0.9 V) (*S*)-enantiomer magnet Up, red curve, is about 1.2±0.02 times larger than the blue (magnet Down) curve, eventually yielding a maximum enantiomeric excess of about 9±1%. The selectivity could in principle be enhanced by using magnetic electrodes with higher spin selectivity, namely magnetic materials with a larger magnetization.

In addition to reduction, spin selectivity can also control oxidation processes. It was shown previously that the electrochemical oxidation of pyrene, and its derivatives, leads to polymerization on metal electrodes.[20] Electropolymerization of 1-pyrenecarboxylic acid was performed on a magnetic electrode (10 nm of Ni and 10 nm of Au on ITO) that was magnetized either Up or Down relative to the electrode surface. The electrochemical polymerization was

carried out in a 2.0 mM solution of pyrene monomer and a fixed potential of 1.68 V versus a silver wire pseudo-reference electrode was applied for 30 min (see Methods for more details). The electropolymerization mechanism was elucidated previously and is described by an $E(CE)_n$ reaction, where E is electron transfer, C is a chemical reaction, and *n* is the degree of polymerization.[21] Fig. 4A shows a reaction scheme for the formation of polypyrene at the 8 position. Initiation of the reaction involves electrooxidation of the monomer unit to form a radical cation. The reaction is then thought to proceed by radical-cation coupling between adjacent monomers, resulting in either dimerization followed by diffusion into solution or polymerization into longer chains on the surface. Note, charge neutrality is maintained through the loss of two protons during the dication-radical intermediate. The steric constraints of the pyrene rings lead to a propeller-like arrangement of the monomers and control over their stereoarrangement imparts axial chirality into the polymer chain.

Fig. 4B shows the CD spectra taken of the pyrene polymer films on the electrode surface. The red curve shows the circular dichroism spectrum with the electrode magnetized in the Up direction and the blue curve corresponds to the case for magnetization in the Down direction. A bare electrode was used as the blank for background subtraction. Note, that the red and blue curves exhibit opposite Cotton effects in pyrene's excimer spectral region. The difference in shape appears to be sample dependent (not field dependent) and may occur because of variation in polymer orientation effects during electrodeposition. Fig. S16 shows a summary of the circular dichroism spectra for different electrodes electropolymerized under the same conditions. An increase in chirality and hence CD intensity may arise from eliminating non-regioregular polymerization pathways.

10.1002/anie.201911400

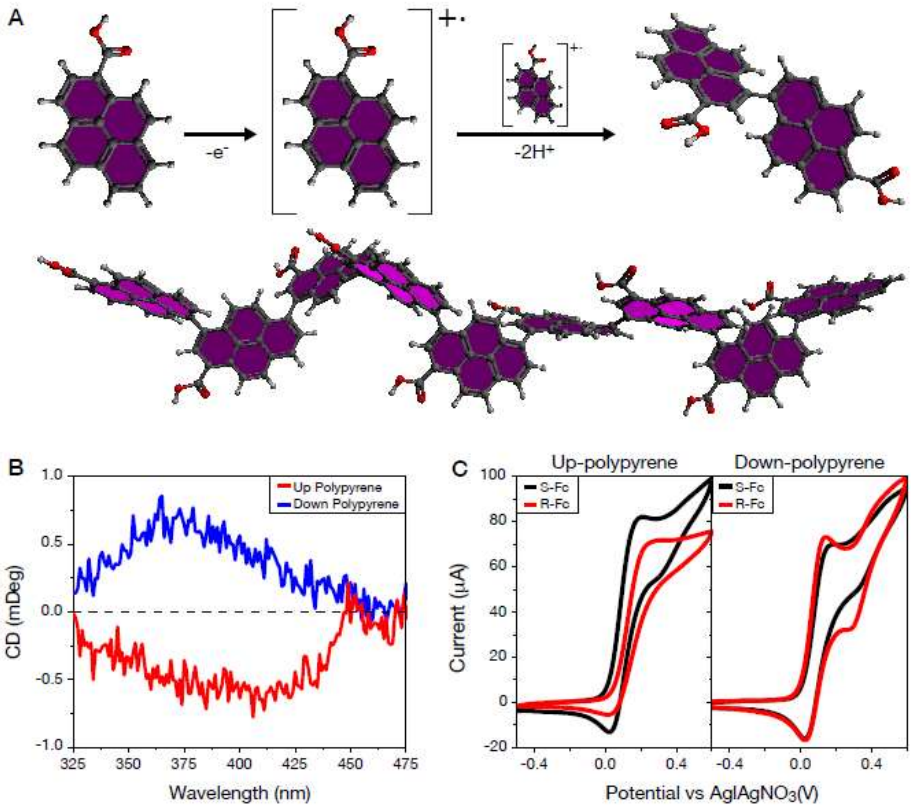

Figure 4. Reaction scheme and chirality in electropolymerized polypyrene. Panel A) shows the reaction scheme for the polymerization of 1-pyrenecarboxcylic acids into polypyrene which exhibits a helical twist (see main text for more details). Panel B) shows circular dichroism spectra for electrodes coated with polypyrene where a magnetic field was applied Up (red) or Down (blue) during electropolymerization. Panel C) shows electrochemistry measurements on (*S*)- (black) or (*R*)-ferrocene (red) with the Up (left) or Down (right) polypyrene-coated working electrodes.

The chirality of the polymer coated electrode was confirmed by performing cyclic voltammetry with a chiral ferrocene (Fc) redox couple, but under no application of a magnetic field. Fig. 4C shows voltammetry data that were collected for two different enantiomerically pure solutions of chiral ferrocene; (*S*)-Fc (black) and (*R*)-Fc (red) using the polypyrene-coated films as working electrodes. The formal potential of the (*S*)-Fc/Fc$^+$ and (*R*)-Fc/Fc$^+$ redox couple occurs at ~0.075 V on a bare Au electrode under these solution conditions (see Methods for more details). The panel on the left shows the case of an electrode in which pyrene electropolymerization was performed with an electrode magnetized in the Up direction and the right panel shows the case for an electrode that was magnetized in the Down direction during electropolymerization. It is evident from the voltammetric peak currents that the Up grown electrode is more sensitive to the (*S*)-Fc,

whereas the Down grown electrode is more sensitive to the (*R*)-Fc. Similar dependencies for redox properties with chiral working electrodes have been reported previously, and further corroborate the chirality demonstrated in the circular dichroism measurements.[22] The difference in current for (*R*)-Fc and (*S*)-Fc is driven by the enantiospecific interactions of the chiral ferrocene and the chirality of the electrode's polypyrene film. Because the chirality of the film may not propagate to the tail end of the polymer, the surface sensitivity to the chiral ferrocene probe can be dampened. This behavior may explain why the asymmetry in (*R*)-Fc and (*S*)-Fc currents is always of the same direction (with respect to polypyrene films grown under a particular magnetic field), but are not always of the same magnitude. Unlike the studies in part 2, the chiral polymer film is more than 200 nm thick and the observed enantioselectivity will have contributions from both the CISS effect and the 'lock-and-key' mechanism.

Conclusion: The findings presented here show that it is possible to manipulate the enantioselectivity in chemical reactions and intermolecular interactions of chiral molecules, by controlling the electron's spin helicity. Because of the relative simplicity of controlling electron spins with a ferromagnetic (or paramagnetic) substrate, these materials were used for inducing enantioselective, electrochemical processes. In contrast to the notion that enantioselectivity requires a chiral reagent molecule or catalyst, this work shows that spin-polarized electrons can provide the chiral bias for enantioselectivity. As electrons are injected from a magnetized electrode into an adsorbed molecule, they have a well-defined spin orientation relative to their velocity; and this spin helicity provides the chiral bias that is required for enantioselective chemical reactions. The results are consistent with former studies in which spin-polarized photoelectrons induced dissociation in enantioselectively.[19] The present study suggests that some past work, exploring enantiospecific processes with chiral electrodes, may also have some contribution from spin-polarized electrons.[22] The studies described above show that the chiral bias provided by the electron helicity is able to drive both oxidation and reduction reactions. In the first case, a spin-polarized achiral SAM enantiospecifically chemisorbed a chiral alcohol from solution, and the SAM thickness was increased systematically to show that the spin polarization, which is injected from a ferromagnetic substrate electrode, only propagates about 0.75 nm. This characteristic length is consistent with the proximity effect observed for diamagnetic films adsorbed on ferromagnets,[23] however it persists even at room temperature for organic SAMs. Enantioselective electrochemical redox reactions of chiral molecules were also demonstrated; generation of an *enantiomeric excess*

from a racemate mixture of chiral molecules. Here we showed that the effect arises from the spin polarization and not from an enantiospecific interaction between the molecules and the FM substrate. In addition, achiral molecules in solution were electropolymerized to form helical polymers, for which the average axial chirality was controlled by the electrode's magnetization direction. In these experiments the only source of chiral bias is that arising from the electron spin asymmetry in the magnetic electrode. Thus enantioselective electrochemistry can be realized for reduction, oxidation, and chemisorption reactions with spin-polarized magnetic electrodes.

The findings presented here demonstrate a new strategy for performing enantioselective chemical reactions, without separating the racemate mixture of the chiral molecules; it provides a new tool for enantioselective synthesis. The results indicate that exchange interaction plays a major role in the enantio-specific interaction between chiral molecules and ferromagnetic substrates. There is still a need for a comprehensive theory that describes this interaction.

Methods:

1. Enantioselective association reaction with spin-polarized monolayers:

The spin-polarized density-of-states from a magnetized Ni surface was used to spin-polarize an adsorbed monolayer film of achiral molecules (carboxyl-terminated alkanethiols) so that they enantiospecifically bind (*S*)- or (*R*)- 1-amino-2-propanol. The magnetic substrate is an ultrathin 5 nm Ni / 10 nm Au film which is magnetized either parallel (Up) or antiparallel (Down). The surface functionalization with COOH terminated alkyl was realized by coating with a self-assembled monolayer (SAM) of carboxyl-terminated alkanethiols [$HS-(CH_2)_{x-1}-COO^-$], which is obtained after 12 hours incubation from a 10mM solution in ethanol.

2. Enantioselective electrochemical redox reactions:

We used (1*R*)-(−)-10-camphorsulfonic acid (CAS Number 35963203) and (1*S*)-(+)-10-camphorsulfonic acid (CAS Number 3144169) directly from Sigma Aldrich to prepare 20 mM racemate solutions in a 0.1 M KCl supporting electrolyte in reagent grade pure water (Millipore). Two types of surfaces of ferromagnetic material using electron-beam evaporation and RF-DC sputtering were prepared: 1) a ferromagnetic film prepared by nickel (150nm) and titanium (10nm) adhesion layer on a silicon (100) substrate (Vin Karola Instrument- Virginia Semiconductor) and 2) a different ferromagnetic surface was prepared with the IBM recipe[11] by using a combination of RF and DC sputtering, with Co and Ni as ferromagnetic material on-top of an aluminum oxide

10.1002/anie.201911400

substrate, with alternate Co (0.3nm) and Ni (0.7nm) for 6 cycles, and with a final 5 nm gold capping layer to avoid oxidation.

3: Enantioselective polymerization from achiral monomers:

ITO substrates (Delta Technologies) were solvent cleaned with ethanol and then oxygen plasma cleaned for 15 minutes using a SPI Plasma Prep II plasma cleaner. The ITO substrates were then secured on top of a silicon wafer with Kapton tape and placed in a MEB550S Plassys Electron Beam Evaporator. A 3nm Ti adhesion layer was evaporated followed by 10 nm of Ni, 3 nm more of Ti, and finally 10 nm of Au to prevent oxidation. The rate of evaporation for Ti, Ni, and Au were 0.02nm/s, 0.2nm/s and 0.05nm/s respectively. The fabricated magnetic electrodes were then attached to a custom made electrochemical cell using General Electric White Silicone II, silicone paste.

Acknowledgment:

We thank Ms. Assunta Green and Dr Pilar Franco from CHIRAL TECHNOLOGIES EUROPE for helping us with the separation procedures. Y.P. acknowledges the support from the Volkswagen Foundation (No. VW 88 367), the Israel Science Foundation (ISF Grant No. 1248/10), the MOS Israel, John Templeton foundation (60796), and last but not least special thanks to Itamar Harel for the immersion device assembly. RN acknowledges the support of the Volkswagen Foundation (No. VW 88 366), the Israel Science Foundation, the MOS Israel, John Templeton foundation (60796), and the Minerva Foundation. DHW acknowledges the support of the John Templeton foundation (60796) and the US National Science Foundation (CHE-1464701).

Author Contributions: TSM, SM, and BPB performed the experiments. GS performed the mass spectrometry and HPLC measurements. JW contributed to the polymerization experiments. SY and FT performed experiments related to part the adsorption and reduction respectively. CF designed and analysed the reduction electrochemical studies. DHW, YP, and RN designed the experiments, analysed the results, and wrote the manuscript.

Additional Information: Additional details on the materials and experimental setup as well as analysis of the molecules are provided in the Supplementary Information.

References

1. L. D., Barron, *Science* **1994**, *266*, 1491-1492.
2. G. L. J. A. Rikken, E. Raupach, *Nature* **1997,** *390*, 493–494.
3. G. L. J. A. Rikken, E. Raupach, *Nature* **2000,** *405*, 932-935.
4. C. Wattanakit, *Curr. Op. Electrochem*., **2017,** *7*, 54–60.
5. B. F. Watkins, J. R. Behling, E. Kariv, L. L. Miller, *J. Am. Chem. Soc.* **1975,** *97*, 3549-3550.
6. H. Maekawa, K. Itoh, S., Goda, I .Nishiguchi, *Chirality* **2003,** *15*, 95–100.
7. L. Dong, et al, *Anal. Chem.*, **2017,** *89*, 9695–9702.
8. I. Mogi, R. Morimoto, R. Aogaki, K. Watanabe, *Scient. Rep.* **2013,** *3*, 2574.
9. M. Gazzotti, et al. *Elect. Acta* **2018,** *286*, 271-278.
10. D. E. Koshland, *Angew. Chem. Int. Ed.*, **1995**, *33*, 2375–2378.
11. K. Banerjee-Ghosh, et. al. *Science* **2018,** *360***,** 1331–1334.

12. A. Kumar, et. al., *PNAS*, **2017,** *114*, 2474–2478.

13. E. Andris, et al, *Angew. Chem. Int. Ed*., **2017,** *56*, 14057 –14060.

14. J. Wang, C. Doubleday, Jr., N. J. Turro, *J. Am. Chem. Soc.*, **1989,** *111*, 3962-3965.

15. R. Naaman, D. H. Waldeck, *Ann. Rev. Phys. Chem*. **2015,** *66*, 263–81.

16. K. Michaeli, N. Kantor-Uriel, R. Naaman, D. H. Waldeck, *Chem. Soc. Rev.* **2016,** *45*, 6478 – 6487.

17 R. Naaman, Y. Paltiel, D. H. Waldeck, *Nature Review Chemistr*y **2019,** *3*, 250-260.

18. B. V. Göhler, et al, *Science* **2011,** *331***,** 894-897.

19. R. A. Rosenberg, D. Mishra, R. Naaman, *Angew. Chemie*, **2015,** *54*, 7295-7298.

20. J. C. Bachman, et al, *Nature Comm.* **2015,** *6*, 7040.

21. R. J. Waltman, J. Bargon, *Canadian J. Chem.*, **1986,** *64*, 76-95.

22. I. Mogi, K. Watanabe, *J. Sol. St. Electrochemistry* **2007,** *11*, 751-756.

23. A. Alija et al, *Phys. Rev. B* **2010,** *82*, 184529.

10.1002/anie.201911400